

*Journal of*  
***Mechanics of  
Materials and Structures***

**THERMOMECHANICAL MODELLING OF FRICTION EFFECTS IN  
GRANULAR FLOWS USING THE DISCRETE ELEMENT METHOD**

Viet Dung Nguyen, Jérôme Fortin, Mohamed Guessasma,  
Emmanuel Bellenger and Claudia Cogné

***Volume 4, N° 2***

***February 2009***



mathematical sciences publishers

## THERMOMECHANICAL MODELLING OF FRICTION EFFECTS IN GRANULAR FLOWS USING THE DISCRETE ELEMENT METHOD

VIET DUNG NGUYEN, JÉRÔME FORTIN, MOHAMED GUESSASMA,  
EMMANUEL BELLENGER AND CLAUDIA COGNÉ

This study deals with the modelling of the thermomechanical phenomena due to friction effects during granular flow. A two-dimensional model using the discrete element method (DEM) and taking into account the contact detection and heat transfers between grains has been developed. Through this study, we have modelled the heat transfer by conductance and the energy dissipation by friction into a granular medium. This modelling enables better understanding of the phenomena at the contact point between grains as well as the energy dissipation by friction of a great number of grains in motion. The validity of the proposed model has been studied by considering some numerical simulations in quasistatic and dynamic regimes.

### 1. Introduction

The published literature analysis has shown the importance of thermal energy in granular media for industrial processes in applications as diversified as powder metallurgy, chemical reactors (catalysts beds), food technology [Laguerre et al. 2006], thermal insulation [Melka and Bézian 1997], or even simply storing particles in a silo after drying [Ketterhagen et al. 2007]. Only few studies are interested in the understanding of heat transfers resulting from thermomechanical effects. However, these complex phenomena with multiphysical characteristics are an essential stake in the world of industry and transports. For instance, strong frictions (braking, jamming) are responsible for half of ignitions of explosive atmospheres, and are also a dreadful cause of fires in vehicles and accidents. One of the difficulties lies in predicting the friction forces and the temperatures in the friction zone based on the intrinsic properties of bodies in contact.

From a thermal energy point of view, sliding contact is the source of a heat generation by friction, whose distribution between the different bodies is difficult to estimate. Besides, the determination of the contact area, which plays an important role in the value of the transferred heat flow, is also difficult to estimate and depends on various parameters like porosity, rugosity, the distribution of contact forces, and the structure of the media. Mechanical engineers are at the origin of the greatest number of works [Slavin et al. 2002; Vargas-Escobar and McCarthy 2002a; Bahrami et al. 2006]. Slavin et al. [2002] and Bahrami et al. [2006] have developed models to estimate the effective thermal conductivity of a particle packing from the intrinsic properties of solids and fluids. These models enable us to determine the apparent thermal conductivity evolution of a granular medium according to the mechanical loading applied to the particle bed. Vargas-Escobar and McCarthy [2002a] have studied more particularly the influence of contact forces on the apparent conductivity of a bed with a small, but finite, area of contact.

*Keywords:* heat transfer, contact, conductance, friction, DEM.

The first part of this work consists of using the discrete element method (DEM) for contact detection, determination of contact forces, and kinematic parameters. A computational program, MULTICOR, that can treat an important number of particles ( $10^6$ ), has been developed to solve the mechanical equations. In the second part, heat transfers by contact as well as energy generation by friction have been studied and implemented in MULTICOR. Finally, through some examples, we underscore the phenomena of thermomechanical interaction.

## 2. Mechanical resolution by DEM

The conventional DEM allows us to model really deformable particles as well as complex shapes, from the ellipsoid to the polygon. Here, we have studied the simple case of nondeformable and nonpenetrable particles in two dimensions with the computational programme MULTICOR [Fortin et al. 2005]. The coordinates and the Euler rotation angles are the configuration parameters  $q$ . The gyroscopic forces are three-dimensional but the centrifugal forces exist even in two-dimensional problems (see Figure 1). The matrix of generalized mass  $M$  of the system doesn't depend on  $q$ , and hence is a diagonal block. The mechanical equation can be written in the form

$$M\ddot{q} = F_{\text{ext}}(q, \dot{q}, t) + R^\alpha,$$

where  $F_{\text{ext}}$  represents the known external forces and  $R^\alpha$  the unknown interior forces related to contact reactions, with  $\alpha$  being the contact number.

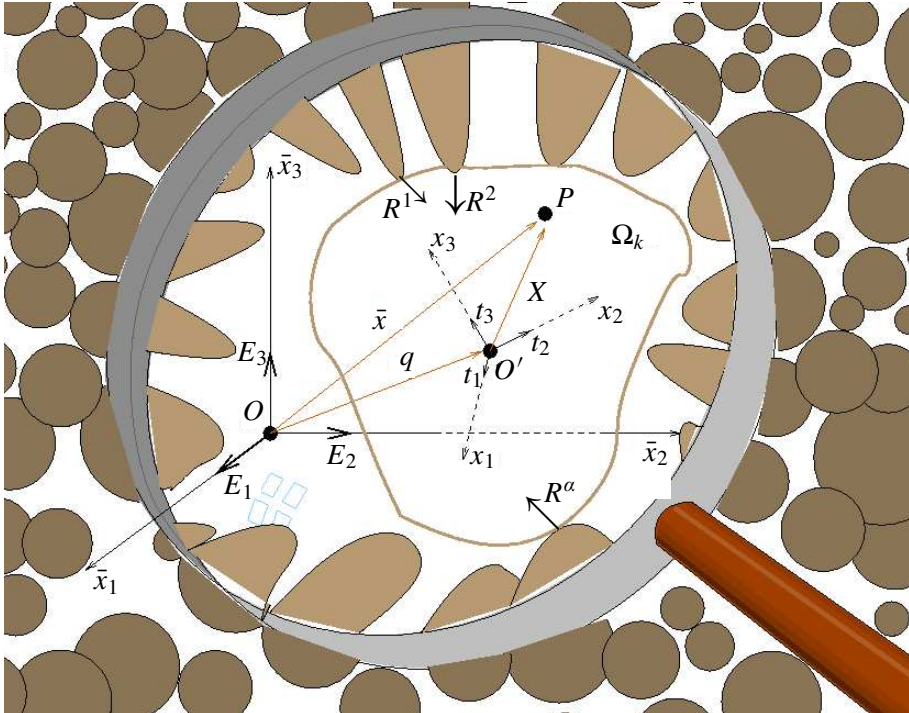


**Figure 1.** Granular media and its kinematic parameters.

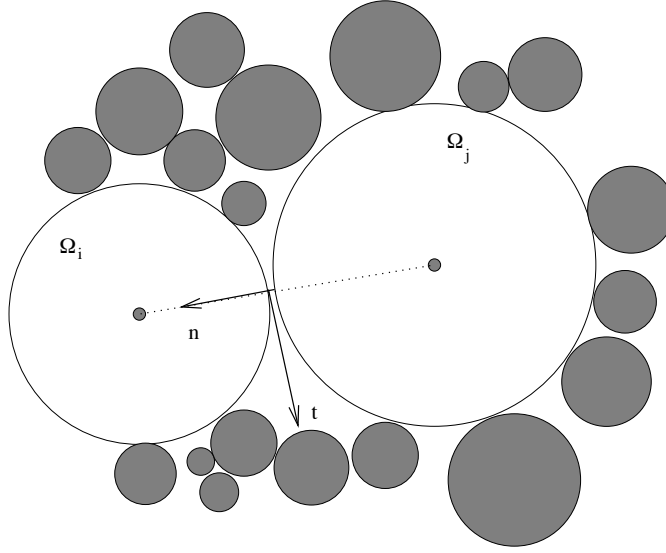


**Figure 2.** Detection of contact.

In a system composed of  $p$  heterogeneous particles (see [Figure 1](#)), the critical parameter for the modelling time is the maximum number of interactions between particles. The more the interaction range is important the more we have to test the possible interactions between particles. MULTICOR uses the partitioning method coupled to a connectivity table [[Fortin and Coorevits 2004](#)]. This technique allows us to reduce the computational time considerably. In this case, the computational time no longer increases as  $O(p^2)$  but only as  $O(p)$ , which is almost optimal. To each pair of particles  $\Omega_i$  and  $\Omega_j$  which may enter in contact, we associated a local reference whose axes are oriented according to the two unit vectors  $n$  and  $t$ , respectively the normal and tangential vectors in the contact plan (see [Figure 2](#)). The normal  $n$  is directed from  $\Omega_j$  to  $\Omega_i$ . The variables put in duality are  $\dot{u}^{ij}$ , the relative local velocity of  $\Omega_i$  with respect to  $\Omega_j$ , and the contact reaction  $r^{ij}$  of  $\Omega_j$  on  $\Omega_i$ . In the local base, they are written as

$$\dot{u}^{ij} = \dot{u}_t^{ij}.t + \dot{u}_n^{ij}.n, \quad r^{ij} = r_t^{ij}.t + r_n^{ij}.n,$$

where  $\dot{u}_n^{ij}$  is the normal separation velocity,  $\dot{u}_t^{ij}$  the sliding velocity,  $r_n^{ij}$  the contact pressure, and  $r_t^{ij}$  the friction force.

The introduction of Coulomb's friction  $\mu$  leads to a nonlinear problem which cannot be solved by a linear programming method. Unlike the usual approach, the bipotential method leads to a single variational principle and an inequality [[Fortin and de Saxcé 1999](#)]. Using Usawa's algorithm, we obtain a resolution algorithm of the constitutive law based on the predictive-corrective scheme expressed by

$$\text{predictor} : \tau^{ij} = r^{ij} - \gamma [\dot{u}_t^{ij} + (\dot{u}_n^{ij} + \mu || - \dot{u}_t^{ij} ||).n], \quad \text{corrector} : r^{ij} = \text{proj}(\tau^{ij}, K_\mu),$$

where  $\gamma$  is a numerical parameter, and  $\tau^{ij}$  the projection of Coulomb's cone  $K_\mu$  leads, according to the value of  $\tau^{ij}$ , to one of the following states: noncontact, contact with friction, or sliding contact. Conventionally, at each time step, the contact forces in the system are determined repeatedly by the method of successive balances based on a Gauss–Seidel algorithm for the two-dimensional version. Each

contact force is calculated by adopting temporary values over the other contacts. The convergence is obtained when the force satisfies the unilateral contact law with dry friction.

The calculation cycle is a time-stepped algorithm which requires the repetition of the following resolution scheme.

$$\left[ \begin{array}{l} t = t + \Delta t \\ \text{Evaluation of the particle positions } q_n \\ \text{Detection of the contact number } \alpha \text{ in the system} \\ \text{Evaluation of the particle velocity (without contact)} \\ \left[ \begin{array}{l} i = i + 1 \quad (\text{iteration of solver bipotential}) \\ \left[ \begin{array}{l} \alpha = \alpha + 1 \quad (\text{contact loop : } \alpha \text{ is the current index of contact}) \\ \text{Evaluation of the contact reactions } r^{\alpha, i+1} \end{array} \right. \\ \text{Indicator of error} \end{array} \right. \\ \text{Evaluation of the velocity} \end{array} \right.$$

### 3. Heat transfer in granular media and thermomechanical formulation

In general, heat transfer in granular media with a stagnant interstitial fluid is assumed to occur by the following physical phenomena:

- Heat conduction through the particles and heat conduction through the fluid between the neighboring particles. Furthermore, in a multicontact system, as considered in this work, we must consider heat conduction through the contact area between two particles  $\Omega_i$  and  $\Omega_j$ . Contact conductance refers to the ability to transmit heat across their mutual interface.
- Radiant heat transfer between the fluid within neighboring voids and radiant heat transfer between the surfaces of neighboring particles. For heat transfer by radiation, contact between surfaces is not required. Radiation is linked to the production of electromagnetic waves by a heat surface.
- For fluids, flow heat transfer by interparticle convection can be considered if there is a difference of temperature between the particles and the fluid.

In frictional granular flow regimes, heat transfer occurs from the phenomena presented above. In addition, it is necessary to consider the heat generated by friction between two particles  $\Omega_i$  and  $\Omega_j$ . Indeed, sliding contact is an important source of heat generation for the dynamic granular problems considered in this work (see [Figure 3](#), left).

In this paper, we assume that conduction through the solid phase dominates the heat conduction. This assumption is verified when

$$\frac{\lambda_s s}{\lambda_f a} \gg 1,$$

where  $\lambda_s$  and  $\lambda_f$  are respectively the conductivities of the particles and the fluid,  $a$  and  $s$  are the radius of the particle and the contact area, respectively.

This expression is satisfied for high thermal conductivity solid materials or for solid particles in a vacuum ( $\lambda_f \rightarrow 0$ ) [[Vargas-Escobar and McCarthy 2002b](#)]. Also, under these conditions, the heat transfer between two adjacent particles  $\Omega_i$  and  $\Omega_j$  is only controlled by the contact conductance. In this work, radiant and convective heat transfers are neglected. Therefore, we only consider heat transfer in granular flow by contact conductance and frictional effects (see [Figure 3](#), right).

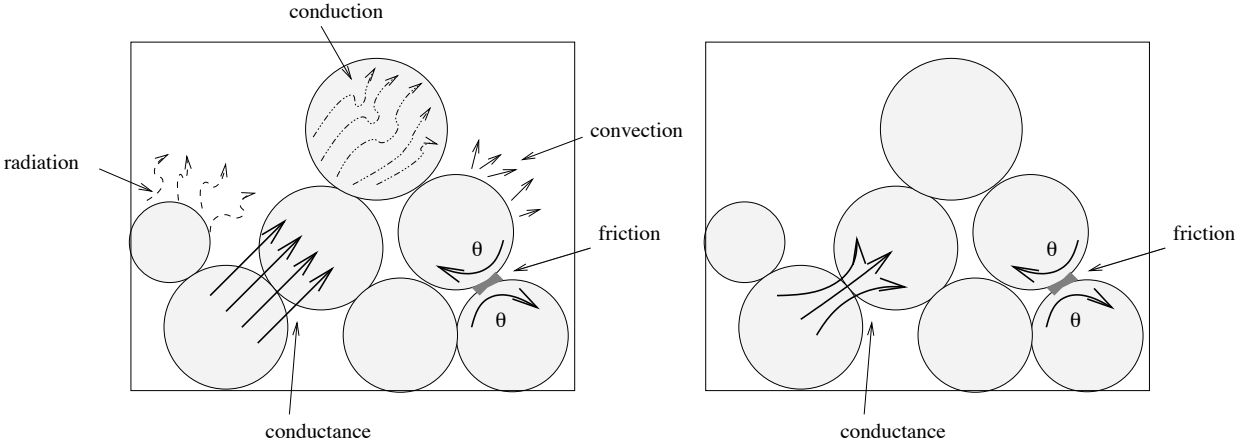


**Figure 3.** Left: heat transfer mechanisms in granular media. Right: heat transfer in MULTICOR.

**3.1. Heat transfer by conductance.** Contact conductance is directly linked to the constriction of the heat flow lines in the contact point [Laguerre et al. 2006]. The thermal contact conductance is defined by the ratio of the heat flow across a contact interface and the magnitude of the temperature discontinuity at the interface,

$$\varphi_{ij} = H_c^{ij}(T_j - T_i),$$

where  $\varphi_{ij}$  is the heat flow transferred between the particles  $\Omega_i$  and  $\Omega_j$ ,  $T_j - T_i$  the temperature difference between the mid-planes of the spheres and  $H_c^{ij}$  the contact conductance between the particles  $\Omega_i$  and  $\Omega_j$ , with  $j$  varying from 1 to the contact number  $\alpha$ .

The coefficient  $H_c^{ij}$ , which is a function of the compression force, refers to the ability of two materials in contact to transfer heat across their mutual interface (see Figure 4). In our work, contact conductance between particles  $\Omega_i$  and  $\Omega_j$  is modeled using Hertz theory as

$$H_c^{ij} = 2\lambda_s \left( \frac{3r_n^{ij} a^*}{4E^*} \right)^{1/3},$$

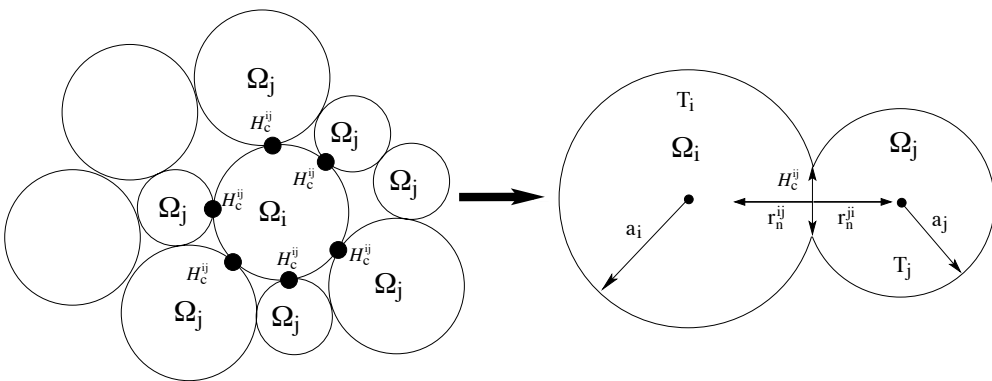


**Figure 4.** Schematic representation of heat transfer by conductance.

where  $r_n^{ij}$  is the normal force,  $a^*$  is the equivalent radius, given by  $\frac{1}{a^*} = \frac{1}{a_i} + \frac{1}{a_j}$ , and  $E^*$  is the effective Young's modulus, so that

$$\frac{1}{E^*} = \frac{1 - \nu_i^2}{E_i} + \frac{1 - \nu_j^2}{E_j},$$

$\nu$  being Poisson's ratio.

The contact between two adjacent particles is assumed to be smooth and sliding. The contact conductance is calculated dynamically at each time step and for all contacts of a particle  $\Omega_i$ .

We recall that the considered particles are nondeformable and nonpenetrable. The use of Hertz's theory only enables us to compute the contact conductance coefficient  $H_c^{ij}$ . We assume that the particles remain rigid all the time.

**3.2. Heat generated by friction.** In this case, heat flow is generated by dissipation of energy during friction between particles. The deformation is neglected because the particles are assumed rigid. Friction is understood as a continuous mechanical solicitation between two bodies. The heat energy generated by friction,  $E_{fij}$ , at the frictional interface during a time step  $\Delta t$  is

$$E_{fij} = \mu \dot{u}_t^{ij} r_n^{ij} \Delta t,$$

where  $\mu$  is the friction coefficient,  $\dot{u}_t^{ij}$  the sliding velocity, and  $r_n^{ij}$  the normal force.

The modelling of the heat generated by friction requires us to share it between particles in sliding contact. Therefore, we define the partition coefficient of generated heat flow  $\beta_{ij}$ . This coefficient depends on different microscopic parameters like the thermal properties, the sliding velocity, heat generation parameters, and the surface roughness if the contact is not perfect [Linck et al. 2006]. Research in this area has proposed different equations to estimate this coefficient. In our study, this coefficient is obtained from the analytical solution of Mokrani and Bourouga [2005],

$$\beta_{ij} = \frac{1}{2} \left( \frac{\rho_i}{\rho_i + \rho_j} + \frac{\lambda_s^i}{\lambda_s^i + \lambda_s^j} \right),$$

where  $\rho$  is the electric resistivity ( $\Omega \text{ m}$ ).

We assume that the packed bed is made of only one material. The partition coefficient of generated heat flow  $\beta_{ij}$  is then equal to  $\frac{1}{2}$ .

**3.3. Thermomechanical resolution.** Taking into account the various phenomena of heat generation mentioned above, the energy balance and the variation of temperature for a particle during a small time step  $\Delta t$  can be written as

$$m_i C_{Pi} \frac{\Delta T_i}{\Delta t} = \sum_{j=1}^{\alpha} \left( H_c^{ij} (T_j - T_i) + \frac{1}{2} \frac{E_{fij}}{\Delta t} \right), \quad (1)$$

where  $m_i$  and  $C_{Pi}$  are the mass and the heat capacity for  $\Omega_i$  respectively, and  $\alpha$  the contact number.

The temperature evolution between two bodies in contact is governed by Equation (1), representing the balance of the heat energy. For static problems this equation is solved with a time step  $\Delta t = 10^{-3}$  s. For dynamical problems (1) is solved with a time step  $\Delta t = 10^{-6}$  s, to assume that the temperature of each particle changes slowly so that thermal perturbations do not propagate further than its immediate

neighbors during one time step. The second requirement is that the heat transfer resistance  $\Omega_i$  (conduction) through a particle is significantly lower than the contact resistance between two particles,  $\Omega_i$  and  $\Omega_j$ , provided that

$$Bi = \frac{H_c^{ij}}{\lambda_s a} \ll 1,$$

where  $Bi$  is the Biot number.

Equation (1) is discretized in order to compute the temperature  $T_i$  at the time step  $t + \Delta t$  as

$$T_i^{t+\Delta t} = T_i^t + \frac{\Delta t}{m_i C_{Pi}} \sum_{j=1}^{\alpha} \left( H_c^{ij} (T_j^t - T_i^t) + \frac{1}{2} \frac{E_{fij}}{\Delta t} \right).$$

The general algorithm implemented in MULTICOR is the following:

$$\left[ \begin{array}{l} t = t + \Delta t \\ \text{Evaluation of the particle positions } q_n \\ \text{Detection of the contact number } \alpha \text{ in the system} \\ \text{Evaluation of the particle velocity (without contact)} \\ \left[ \begin{array}{l} i = i + 1 \quad (\text{iterations of solver bipotential}) \\ \left[ \begin{array}{l} \alpha = \alpha + 1 \quad (\text{contact loop}) \\ \text{Evaluation the contact reaction } r^{\alpha, i+1} \end{array} \right] \\ \text{Indicator of error} \end{array} \right] \\ \text{Evaluation of } T_i^t, H_c^{ij}, E_{fij} \\ \text{Evaluation of the temperature } T_i^{t+\Delta t} \\ \text{Evaluation of the velocity} \end{array} \right.$$

The resolution of the heat problem requires us to compute at each time step the contact detection, the determination of forces, and the velocities of particles.

## 4. Numerical simulations

**4.1. Comparison between DEM and FEM.** The first application was carried out on a particulate system obtained by a triangular arrangement of 14 particles, with an identical size and a circular shape (1 mm radius). We initially suppose that particle 1 is heated at 100° C and the remaining particles are at a temperature of 20° C (see Figure 5).

From the thermal point of view, this simple modelling allows us to study the diffusion of the heat flow by conductance in granular media. In order to check that this assumption is not too restrictive, we compared MULTICOR's prediction with the results obtained by CAST3M software based on the finite element method (FEM) (see Figure 5). Through this comparison, we could check that the thermal resistance within particles was negligible compared to the thermal contact resistance between particles. This hypothesis could be checked by studying the temperature evolution in particles 1, 5 and 14. The good agreement between MULTICOR and CAST3M seems to validate the assumption about the heat transfer occurring only by conductance.

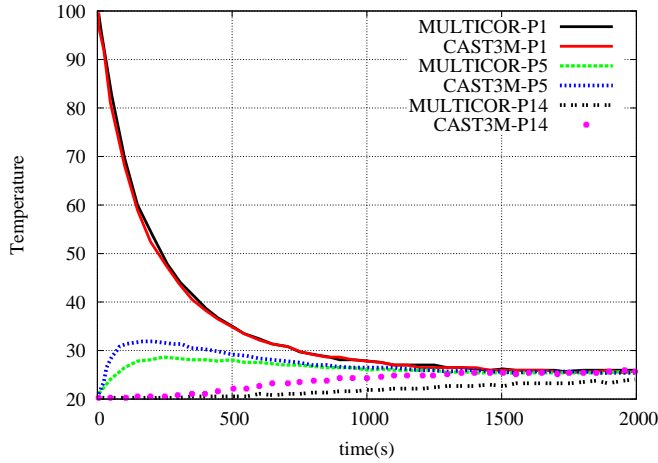


**Figure 5.** Temperature evolution in particles 1, 5, and 14 obtained by MULTICOR and CAST3M.

**4.2. Comparison between experiment and MULTICOR prediction.** In order to validate our thermomechanical model implemented in MULTICOR, we have compared the results with experimental data from [Vargas-Escobar and McCarthy 2002b]. In this study, the authors developed an experimental setup to investigate the heat transfer in a quasistatic configuration. The system is composed of dispersed stainless steel spheres forming a two-dimensional packed bed ( $30.4 \times 45.7 \text{ cm}^2$ ). The bottom wall is kept at  $T_{\text{wall}} = 50^\circ \text{C}$ . The top, left, and right walls are insulated (see Figure 6, left). The initial temperature is  $T_0 = 25^\circ \text{C}$ .

The DEM model shown in the figure was computed by using the thermomechanical properties of stainless steel based on experiments (see Table 1).

In Figure 6, right, we present a part of thermal map after 30 minutes heating. The temperature in the heated granular bed does not propagate uniformly. The front oscillates as force chains appear and disappear along the bed’s height.

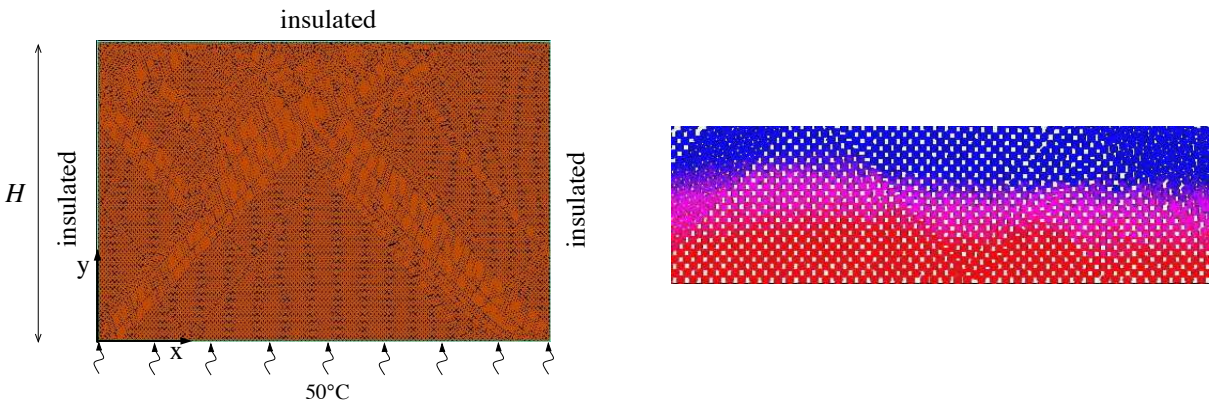


**Figure 6.** Left: the MULTICOR model. Right: part of the thermal map after 30 minutes heating.

Density	Poisson's ratio	Young's modulus	Particle radius	$\lambda_s$
7,500 kg/m <sup>3</sup>	0.29	193 GPa	0.003 m	15 W/mK
Number of particles	Length	Height	Friction coefficient	
15,548	0.45 m	0.31 m	0.29	

**Table 1.** Parameters used in the simulation.

Figure 7 presents a comparison of the temperature as a function of bed's height given by our predictions and the experimental results obtained by Vargas et al. [2002b] after 30 minutes heating. In this figure,  $\theta$  represents the dimensionless temperature and  $\eta$  the dimensionless height, given by the equations

$$\theta = \frac{T - T_0}{T_{\text{wall}} - T_0}, \quad \eta = \frac{y}{H}.$$

As shown in Figure 7, the predicted temperature is less accurate for the particles at the bottom of the bed. However, it can be seen that the simulation results matches the experimental curves for dimensionless heights higher than 0.03, which allows us to validate the model prediction in the quasistatic case.

**4.3. Simulation of heat generation by friction in granular media.** In this part, we begin to investigate the problem of heat generation in the granular material subjected to shearing solicitation at an imposed velocity. Two cases of shearing will be studied: the quasistatic and dynamic regimes.

The granular material consists of  $p$  particles having diameters  $d$  (1, 2, and 3 mm). The intergranular contact is characterized by the friction coefficient  $\mu = 0.5$ .

In the geometry of the shearing plane (see Figure 8), the material is compacted by gravity between two rough parallel walls at a distance  $H$ . The top wall is set in motion with velocity  $V$  in the positive  $x$  direction, and the system is compressed by imposing a uniaxial load  $F$ . Periodic conditions are imposed at the lateral boundaries. This means that a particle leaving through one of the boundaries reenters the

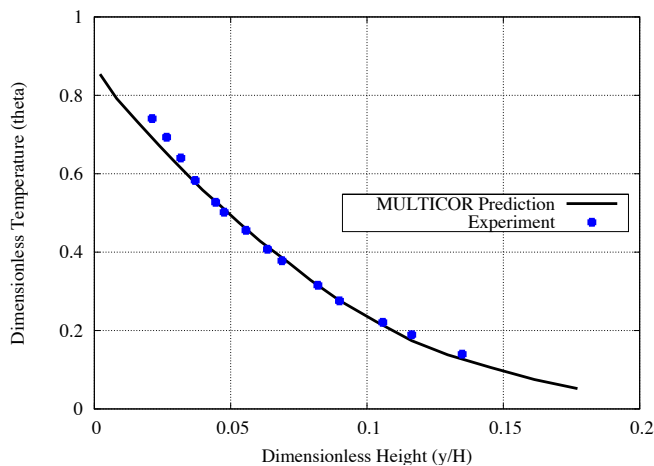


**Figure 7.** Comparison of experimental data with MULTICOR results after 30 minutes heating.

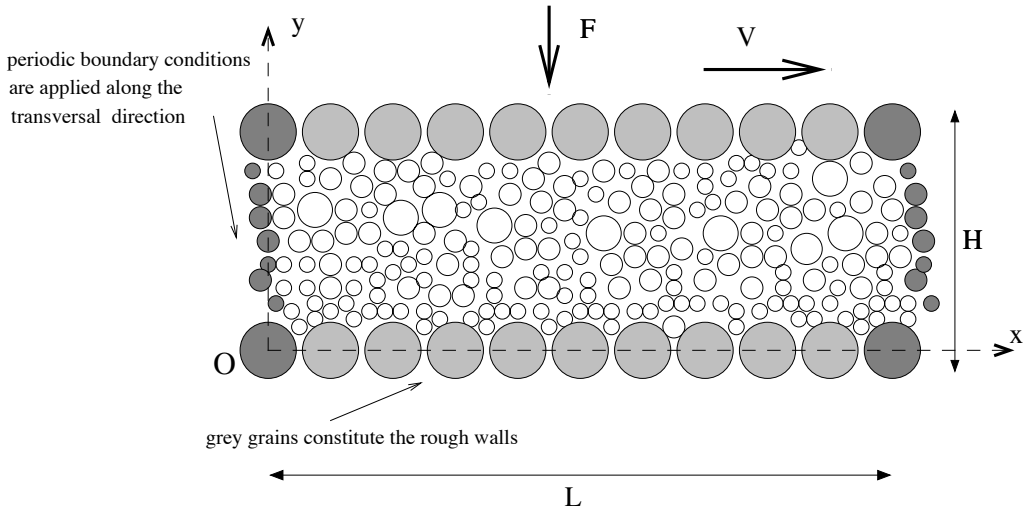


**Figure 8.** Model of shearing plan with periodic boundaries.

cell at the same vertical location and with the same kinematic and dynamic conditions.  $L$  is the length of the simulated flow (equal to 40 particles). This size appears sufficient to neglect the length effects of the simulation box. It is considered here that the roughness of wall surface is modeled by jointed grains having the same characteristics as grains in the flow.

Conventionally, we observe two regimes in granular flows. First we have the quasistatic regime, which usually obeys the constitutive laws in which the effective friction coefficient is constant. Secondly, there is the rapid-flow or dynamic regime, where the particles interact collisionally. In this case, the solid fraction is close to the maximum.

In [Figure 9](#) we present the velocity field of two regimes. On the top two images we note the appearance of small vortices which characterize the quasistatic regime. These disappear in the dynamic regime, observed in the bottom images. In this case, the granular flow becomes stationary. This phenomenon gives us a better understanding of the behavior of granular flow [[da Cruz 2004](#)].

[Figure 10](#) shows the contact force distribution across the granular material at the beginning of the simulation and when the stationary regime is established.

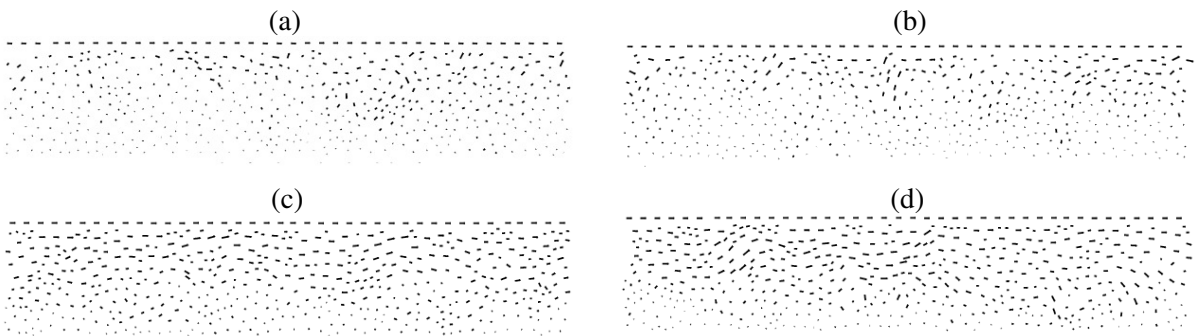


**Figure 9.** The velocity field in the quasistatic regime with a small vortex (top row), and in the dynamic regime (bottom).

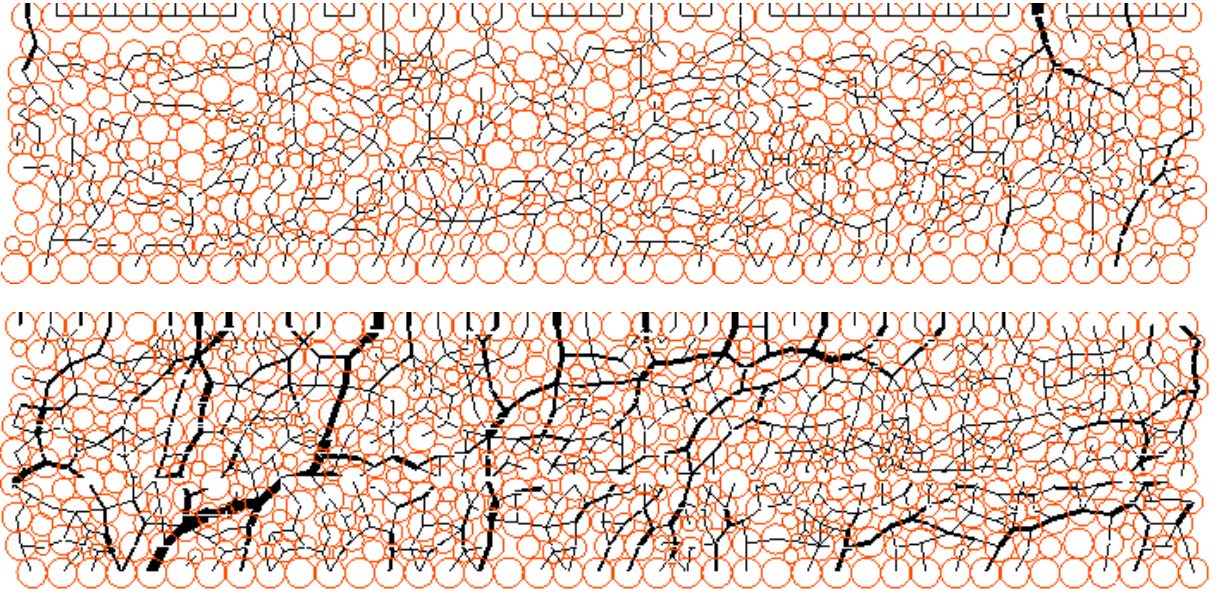


**Figure 10.** Contact forces field at the beginning of the simulation (top) and when stationary flow is established (bottom).

Another result is concerned with the variation of velocity as a function of the height. We see in Figure 11 that the average velocity agrees well with the curves proposed by da Cruz [2004], [?], and Vargas-Escobar [2002]. There is no turbulence close to the mobile wall.

The major result of this work is the heat generated by friction between particles and the shearing wall (see Figure 12). Figure 13, left, shows how heat varies with the granular layer depth. The hottest zone is located in the middle of the flow. These observations are confirmed by Vargas-Escobar [2002], who has shown that the granular temperature profiles illustrate the high-shear zones in the center of the cell.

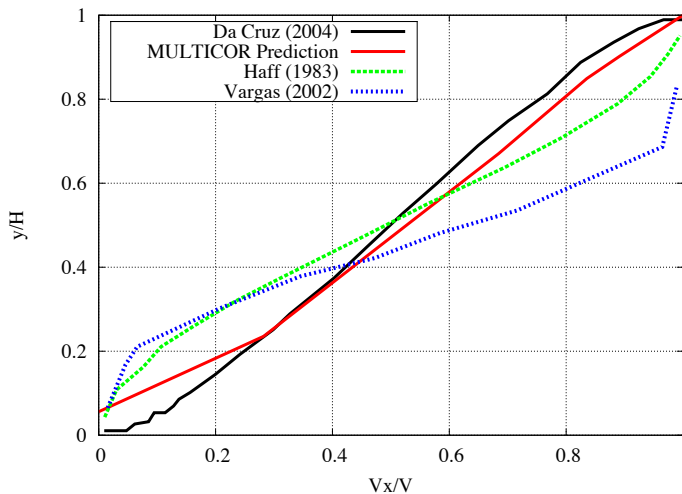


**Figure 11.** Typical velocity normalized profile.

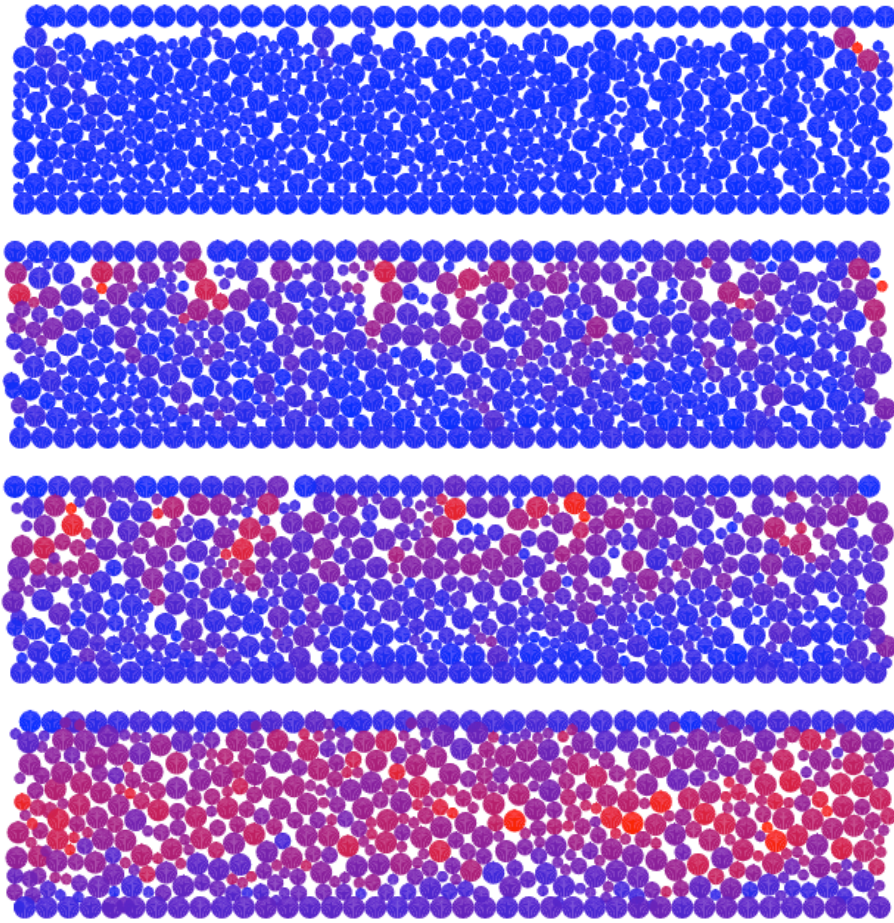


**Figure 12.** Thermal maps of heat evolution in the quasistatic regime.

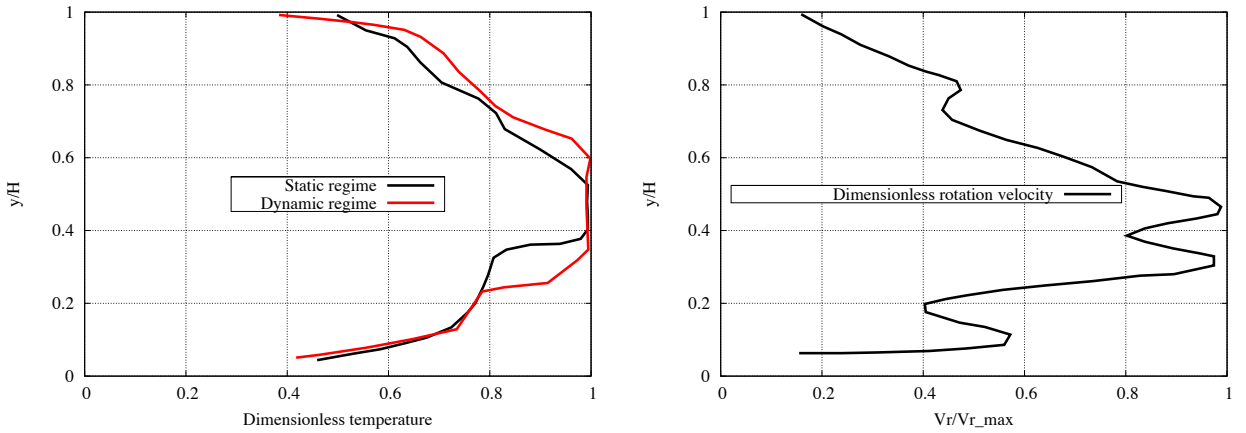


**Figure 13.** Left: heat profiles. Right: normalized angular velocity.

Here we note that thermal symmetry of the heat profile means that the bottom wall plays an important role in the heat generation. We also note that these profiles correspond with the angular velocity curves, seen on the right in [Figure 13](#).

## 5. Conclusions

The present work focuses on the modelling of heat transfer and heat generation by friction in a granular material by using DEM. The proposed model has been implemented in MULTICOR software and performed for some examples to check its validity. The numerical predictions obtained with MULTICOR agree with the experimental results and numerical predictions from the literature. Therefore, the proposed assumptions about the predominance of heat transfer by conductance in comparison with other thermal effects has negligible influence on the numerical predictions.

The next step will consist in the incorporation of the other heat transfer phenomena like convection, radiation, and impact effect. Moreover, further studies will focus on the dynamic friction coefficient and its changes with the temperature and the wear in the contact area. An experimental campaign is also planned with our industrial partner [Proust et al. \[2007\]](#).

## Acknowledgement

We thank Mrs. Boutinaud-Morel for her advice in the translation of this article.

## References

- [Bahrami et al. 2006] M. Bahrami, M. M. Yovanovich, and J. R. Culham, “Effective thermal conductivity of rough spherical packed beds”, *Int. J. Heat Mass Tran.* **49**:19-20 (2006), 3691–3701.
- [da Cruz 2004] F. da Cruz, *Écoulement de grains secs: frottement et blocage*, Ph.D. thesis, École Nationale des Ponts et Chaussées, Paris, 2004.
- [Fortin and Coorevits 2004] J. J. Fortin and P. Coorevits, “Selecting contact particles in dynamics granular mechanics systems”, *J. Comput. Appl. Math.* **168**:1-2 (2004), 207–213.
- [Fortin and de Saxcé 1999] J. Fortin and G. de Saxcé, “Modélisation numérique des milieux granulaires par l’approche du bi-potentiel”, *C. R. Acad. Sci. IIb* **327** (1999), 721–724.
- [Fortin et al. 2005] J. Fortin, O. Millet, and G. de Saxcé, “Numerical simulation of granular materials by an improved discrete element method”, *Int. J. Numer. Meth. Eng.* **62**:5 (2005), 639–663.
- [Haff 1983] P. K. Haff, “Grain flow as a fluid- mechanical phenomenon”, *J. Fluid Mech.* **134** (1983), 401–430.
- [Ketterhagen et al. 2007] W. R. Ketterhagen, J. S. Curtis, C. R. Wassgren, A. Kong, P. J. Narayan, and B. C. Hancock, “Granular segregation in discharging cylindrical hoppers: a discrete element and experimental study”, *Chem. Eng. Sci.* **62**:22 (2007), 6423–6439.
- [Laguerre et al. 2006] O. Laguerre, S. B. Amara, and D. Flick, “Heat transfer between wall and packed bed crossed by low velocity airflow”, *Appl. Therm. Eng.* **26**:16 (2006), 1951–1960.
- [Linck et al. 2006] V. Linck, A. Saulot, and L. Baillet, “Consequence of contact local kinematics of sliding bodies on the surface temperatures generated”, *Tribol. Int.* **39**:12 (2006), 1664–1673.
- [Melka and Bézian 1997] S. Melka and J. J. Bézian, “L’isolation thermique par les matériaux granulaires”, *Rev. Gen. Therm.* **36**:5 (1997), 345–353.
- [Mokrani and Bourouga 2005] H. Mokrani and B. Bourouga, “Modèle de coefficient de partage du flux généré à une interface de contact électrothermique: approche microscopique en régime permanent”, in *12èmes Journées Internationales de Thermique* (Tanger, Morocco, 2005), 2005.

- [Proust et al. 2007] C. Proust, S. Hawksworth, R. Rogers, M. Beyer, D. Lakic, D. Raveau, P. Hervé, V. Pina, C. Petitfrère, and X. Lefebvre, “Development of a method for predicting the ignition of explosive atmospheres by mechanical friction and impacts (MECHEX)”, *J. Loss Prevent. Proc.* **20**:4-6 (2007), 349–365.
- [Slavin et al. 2002] A. J. Slavin, V. Arcas, C. A. Greenhalgh, E. R. Irvine, and D. B. Marshall, “Theoretical model for the thermal conductivity of a packed bed of solid spheroids in the presence of a static gas, with no adjustable parameters except at low pressure and temperature”, *Int. J. Heat Mass Tran.* **45**:20 (2002), 4151–4161.
- [Vargas-Escobar 2002] W. L. Vargas-Escobar, *Discrete modeling of heat conduction in granular media*, Ph.D. thesis, University of Pittsburgh, Pittsburgh, 2002, Available at <http://etd.library.pitt.edu/ETD/available/etd-02012002-193942/unrestricted/FinalBW.pdf>.
- [Vargas-Escobar and McCarthy 2002a] W. L. Vargas and J. J. McCarthy, “Conductivity of granular media with stagnant interstitial fluids via thermal particle dynamics simulation”, *Int. J. Heat Mass Tran.* **45**:24 (2002), 4847–4856.
- [Vargas-Escobar and McCarthy 2002b] W. L. Vargas-Escobar and J. J. McCarthy, “Stress effects on the conductivity of particulate beds”, *Chem. Eng. Sci.* **57**:15 (2002), 3119–3131.

Received 17 Dec 2007. Accepted 7 Mar 2008.

VIET DUNG NGUYEN: [vietdung.nguyen@u-picardie.fr](mailto:vietdung.nguyen@u-picardie.fr)

Laboratoire des Technologies Innovantes (EA 3899), Université de Picardie Jules Verne, IUT de l’Aisne, 02100 Saint Quentin, France

JÉRÔME FORTIN: [jerome.fortin@insset.u-picardie.fr](mailto:jerome.fortin@insset.u-picardie.fr)

Laboratoire des Technologies Innovantes (EA 3899), Université de Picardie Jules Verne, IUT de l’Aisne, 02100 Saint Quentin, France

MOHAMED GUESSASMA: [mohamed.guessasma@u-picardie.fr](mailto:mohamed.guessasma@u-picardie.fr)

Laboratoire des Technologies Innovantes (EA 3899), Université de Picardie Jules Verne, IUT de l’Aisne, 02100 Saint Quentin, France

EMMANUEL BELLENGER: [emmanuel.bellenger@u-picardie.fr](mailto:emmanuel.bellenger@u-picardie.fr)

Laboratoire des Technologies Innovantes (EA 3899), Université de Picardie Jules Verne, IUT de l’Aisne, 02100 Saint Quentin, France

CLAUDIA COGNÉ: [claudia.cogne@u-picardie.fr](mailto:claudia.cogne@u-picardie.fr)

Laboratoire des Technologies Innovantes (EA 3899), Université de Picardie Jules Verne, IUT de l’Aisne, 02100 Saint Quentin, France